

AD P 0 0 1 0 9 5

AN AIRBORNE ROTMAN LENS PHASED ARRAY

Kenneth Ewen and Gary D. Brunner

Goodyear Aerospace Corporation

Arizona Division

Litchfield Park, Arizona 85340

ABSTRACT

An airborne single axis phased array has been designed using a folded Rotman Lens as a cost and performance effective alternative to a phase shifter steered array.

Significant aircraft space and weight restrictions were met by use of a folded parallel plate lens for power division and beam steering in the azimuth plane and air stripline for power division in the elevation plane. Mechanical design of the antenna emphasized producibility of the components using numerically-controlled milling machines and repetitive assembly techniques.

1. INTRODUCTION

Airborne radars in reconnaissance, guidance, and weapon delivery modes are placing increasingly severe requirements on antennas, including wide instantaneous and total bandwidths, wide angle beam scan, selectable beamwidths, and sidelobe control. These requirements must be met in the face of aircraft volume, weight, and environmental restrictions that call for unique solutions.



In particular, synthetic aperture radar (SAR), which has been used in Goodyear Aerospace Corporation-produced operational reconnaissance radars such as the AN/UPD-8 since the mid 1960s, will be used in fire control, weapon delivery, and higher performance reconnaissance radars. Instantaneous bandwidths in excess of 100 megahertz (MHz) will be required for range resolution; wide angle scan will provide aircraft motion compensation, target acquisition, tracking and identification; and sidelobe control will be necessary for aircraft survivability.

The next generation reconnaissance aircraft will have interchangeable pods holding a variety of sensors. Antennas must be compatible with pod diameters, compete with other electronics for area and location, and operate in a nonpressurized environment over temperature extremes.

Phased arrays have promised to satisfy many of the requirements, but have been plagued by cost, weight, environmental, power, and performance problems.

This paper will describe a Goodyear Aerospace-sponsored Rotman lens phased array suitable as a prototype for an antenna for a pod-mounted reconnaissance radar. This single axis scanned array offers a cost-effective alternative to a phased array, and for wideband systems can provide superior performance.

2. PERFORMANCE REQUIREMENTS

On the basis of assumptions made regarding the performance requirements of future reconnaissance radars a set of minimum antenna

performance requirements was generated which are representative of the requirements for an advanced pod-mounted system operating in X-band. The results are presented in Table 1. Also considered were the physical and environmental constraints imposed by a pod installation which are presented in Table 2.

3. CONCEPTUAL DESIGN

3.1 General - In anticipation of the operational needs of next generation reconnaissance radars Goodyear Aerospace sponsored a study to define an

TABLE 1 - MINIMUM ANTENNA REQUIREMENTS

Gain	≥ 33 dB
Azimuth beamwidth	≤ 1.8 deg
Azimuth sidelobes	≤ -18 dB
Azimuth beam pointing	± 20 deg both sides of aircraft
Elevation beamwidth	Shaped or selectable
Elevation sidelobes	≤ -13 dB
Elevation beam pointing	± 25 deg both sides of aircraft
Instantaneous bandwidth	$= 120$ MHz

TABLE 2 - PHYSICAL ANTENNA CONSTRAINTS

Volume	27-in.-dia x 72-in.-long cylinder
Weight	≤ 250 pounds (lb)
Altitude	$\leq 40,000$ feet (ft)
Temperature	-65 deg Centigrade (C) minimum, +125 deg C maximum

optimum antenna approach for these applications. Tradeoffs were performed among various antenna types including mechanically steered reflectors and arrays and electronically scanned arrays (ESAs). The outcome of this effort was a concept for a lens-fed planar array which achieved azimuth scanning through the motion of a small feed horn within the antenna envelope. By realizing beam scanning without physically steering the antenna, the swept volume demands of the antenna were minimized and the available aperture was maximized. By relying on a mechanical approach the cost/complexity penalties of electronic scanning were avoided. The true time delay nature of the scanning produced in this manner and reliance on TEM propagation paths throughout the lens results in an inherently wide bandwidth.

Elevation beam steering would be accomplished by conventional roll axis control and elevation beam selection is employed in preference to beam shaping because of the left/right look direction requirement. The advantages offered by this concept were sufficiently compelling to warrant development of a prototype model with the antenna performance requirements set forth earlier serving as performance objectives. A drawing of the prototype concept illustrating the key development areas is shown in Figure 1.

3.2 Lens Concept - The backbone of the candidate approach is the wide angle constrained microwave lens used to feed the planar array. Constrained microwave lenses are characterized by the fact that they do not obey Snell's Law, the feature which results in their wide angle scanning

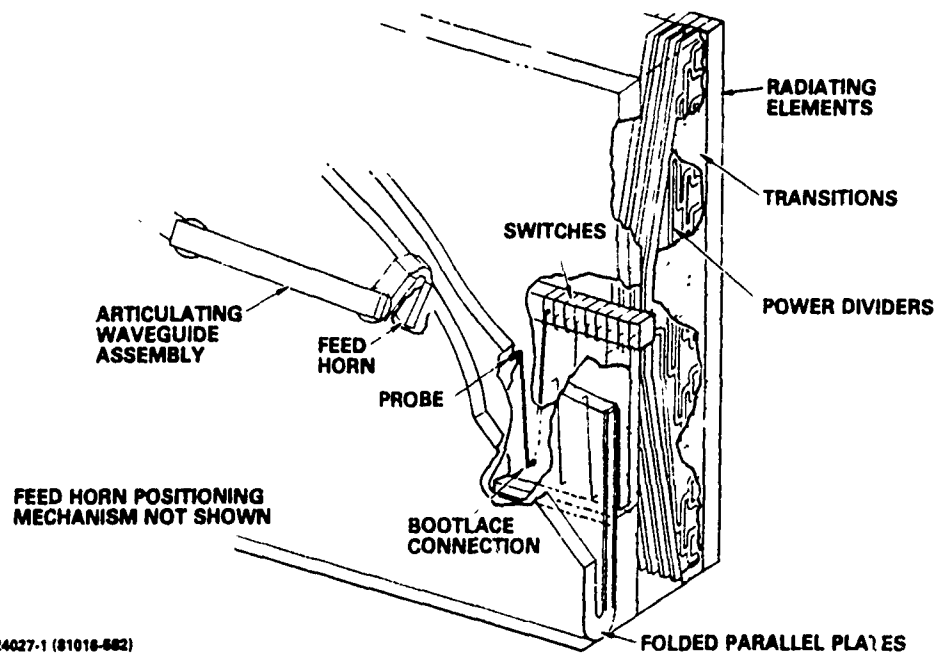


Figure 1 - Rotman Lens Phased Array

properties. Snell's Law is circumvented by establishing fixed path lengths (transmission line connections) between corresponding points on the two surfaces (or contours) of the lens. Under these conditions lens performance becomes dependent on specification of the inner and outer lens contours, the path length variation and position within the lens, and the focal path. Ruze¹ studied constrained lenses having collinear constant electrical length paths between inner and outer lens faces which produced a lens design having two points of perfect focus located symmetrically with respect to the axis. A lens configuration offering performance advantages over the Ruze type was investigated by Rotman and Turner². Figure 2 depicts the Rotman lens configuration schematically using his notation. The optimum focal path for the Rotman lens is a circular arc, R , passing through the three perfect focal points, F_1 , G , and F_2 .

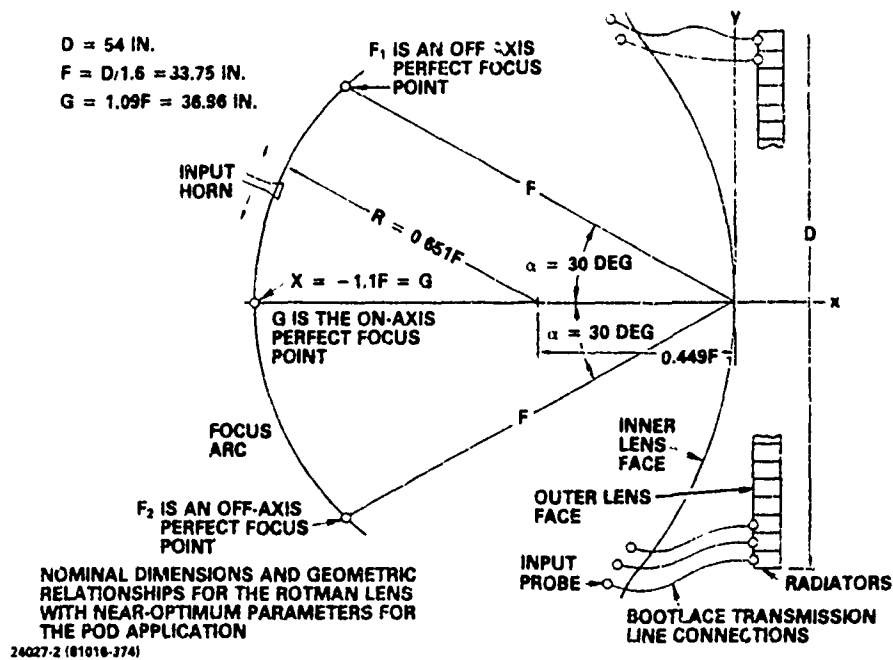


Figure 2 — Rotman Lens Concept

4. IMPLEMENTATION

4.1 Block Diagram - A functional description of the main developmental areas associated with implementation of the Rotman lens phased array is presented here, with a more detailed discussion of design considerations following.

The radiating aperture is a 54-in. long by 13-in. high assembly of 80 vertical radiators. Each vertical radiator consists of 20 contiguous open-ended waveguide elements joined on their narrow walls and is connected to a power divider assembly containing one 16-way and one four-way corporate power divider network, and a three-way switch. The 20 outputs of the power divider network transition to the 20 waveguide

elements of the vertical radiator. The three-way switch permits selection of either 4-, 16-, or 20-element vertical apertures.

The input of each vertical power divider assembly connects to the output of a "bootlace" lens element, a length of semirigid coaxial cable cut to a dimension determined from the lens design equations based on its position within the aperture. The input end of the bootlace lens is in turn connected to the output of the parallel plate region through an array of E-field probes extending into the parallel plate region along a contour, and at intervals, specified by the lens design. The parallel plate region is terminated by a reflecting surface behind the probe array which corresponds to the inner lens contour.

To accommodate the 37-in. focal length of the lens within the 27-in. dia allocated to the antenna, the parallel plates are folded. The input end of the parallel plate region is open to permit traversal by the feed horn which illuminates the lens. The H-plane feed horn extends into the parallel plate region and travels on a track mounted to an outer surface of the parallel plates with a contour corresponding to the focal arc of the lens system. The feed horn is driven by a direct current (DC) torque motor through a steel band drive. Position is controlled by a feedback loop and position sensing is accomplished by means of a linear sensor mounted directly to the drive track. Connection of the microwave signal to the moving feed horn is through an articulating waveguide assembly comprised of three rotary joints and interconnecting waveguide. A stationary waveguide run connects the articulating waveguide assembly with the antenna

input through a roll axis rotary joint in the rear mounting plate. A DC torque motor provides the roll axis drive. Mounting of the antenna is by means of forward and aft mounting plates. The antenna is enclosed in a thin-walled composite cylinder for pressurized operation in a nonpressurized pod.

Overall antenna length including the fore and aft mounting plates is 68 in. The maximum diameter is 25 in. at the rear plate. The microwave section is 13.5-in. deep including feed waveguide and will roll within a 10.7-in. radius.

Front and rear views of the antenna are shown in Figure 3. The front view shows the radiating array and the vertical power dividers, while the rear view is of the complete antenna less the pressure cylinder and forward mounting plate. Figure 4 is a section through the vertical midplane of the antenna showing the foiled lens, bootlace cables, and vertical assembly relationships.

4.2 Lens System Design -

4.2.1 Lens Parameters - The choice of lens parameters will depend upon the design scan angles, maximum desired scan angle, lens depth, and number of radiators and can be established by analysis². In addition, the aperture illumination as a function of the feed horn, lens output curve, and scan angle must also be considered.

The antenna azimuth dimension had been fixed at 54 in. by available mechanical space, with a total of 80 radiators from radiator voltage standing wave ratio (VSWR) calculations. Additional tradeoffs established that

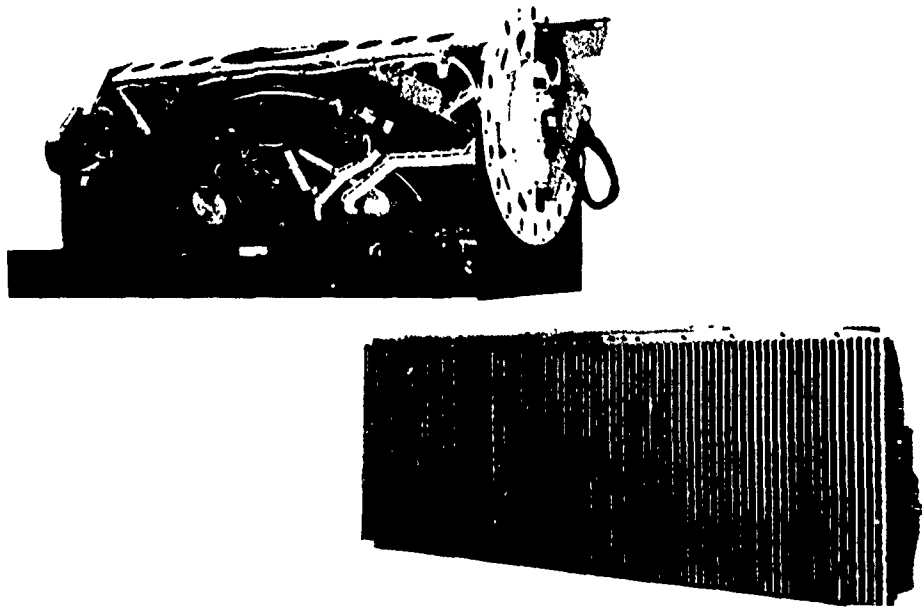
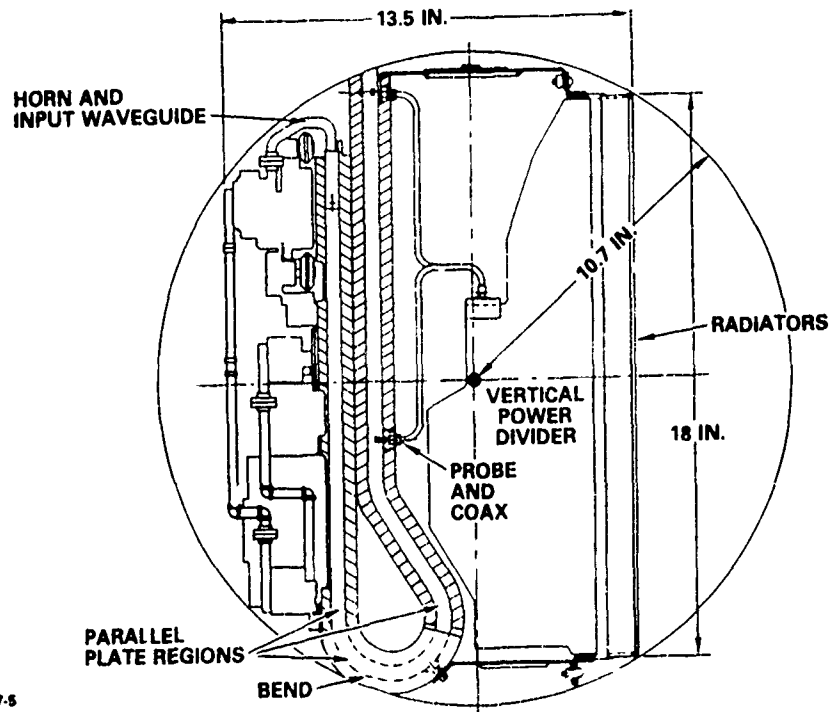


Figure 3 - Rotman Lens Phased Array Antenna



24027-5

Figure 4 - Antenna Cross Section

$G = 36.956$ in., $F = 33.75$ in., and $\alpha = 30$ degrees would provide acceptable aperture phase errors for all scan angles over a 0 to ± 38 -deg region and a mechanical geometry suitable for folding.

Additional calculations were made of sidelobes, beamwidth, and gain loss expected for various scan angles and feed horn aperture. Typical data is shown in Figure 5 and the expected antenna performance for the selected horn dimensions is given in Figure 6. Performance obtained with the 2-in. aperture horn was considered a best compromise between beamwidth, sidelobe, and relative gain loss, based upon expected overall radar performance.

Calculations were also performed to establish feasibility of a low sidelobe (≈ 40 dB) antenna, and while the data indicated that this level was achievable, a low sidelobe design was not pursued on this effort.

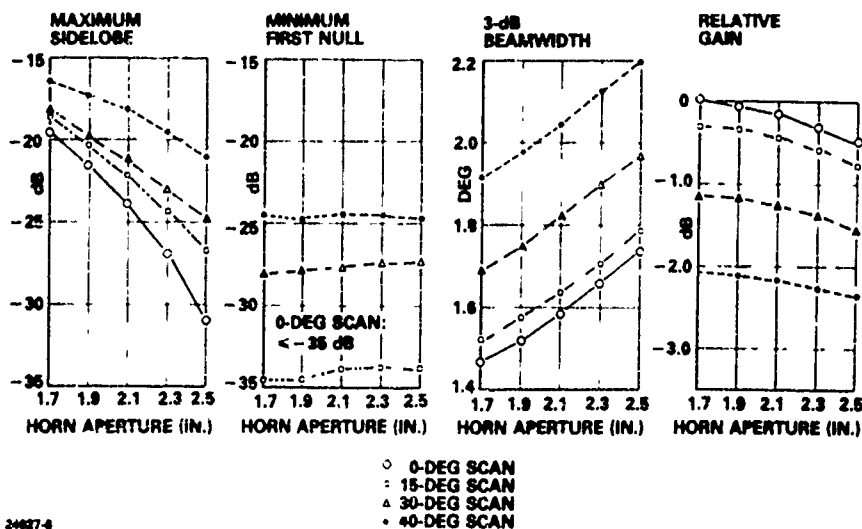


Figure 5 - Computed Lens Performance for Horn Feed

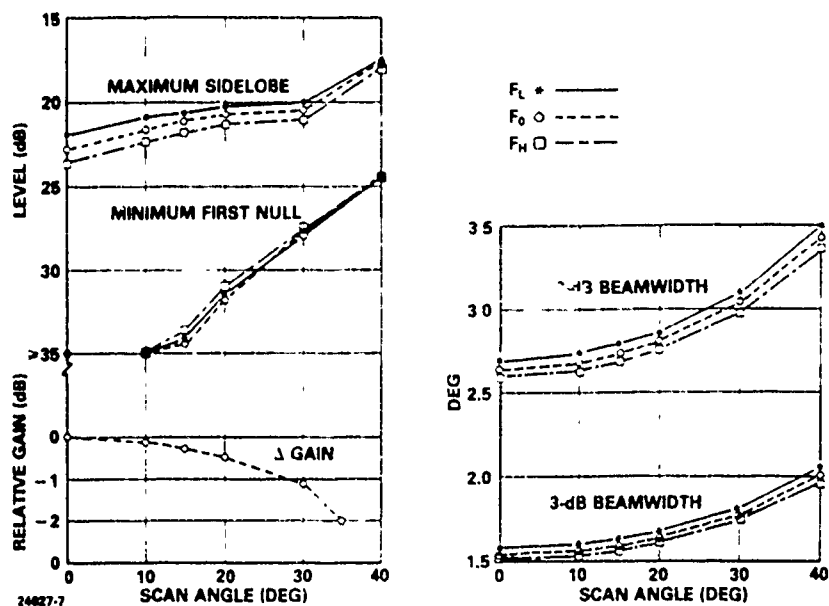


Figure 6 - Expected Performance for Selected Feed

4.2.2 Lens Output Probes and Cables - The output probes in a Rotman lens are not uniformly spaced, but rather are a function of radiator location from the centerline. The spacings for this design are shown in Figure 7.

Large spacings on the edge probes can lead to a grating lobe being generated internally in the parallel plate region which would degrade the radiated pattern and gain data. The incidence angle at which the grating lobe will enter visible space is

$$\theta_i = \sin^{-1} \left[\frac{\lambda}{S} - 1 \right], \quad (1)$$

where S is the average spacing to the adjacent probes.

Incidence angles between each probe and the horn are shown in Figure 8 for four scan angles. The use of this data and Equation (1) established that no more than four probes up to a scan angle of 30 deg and six

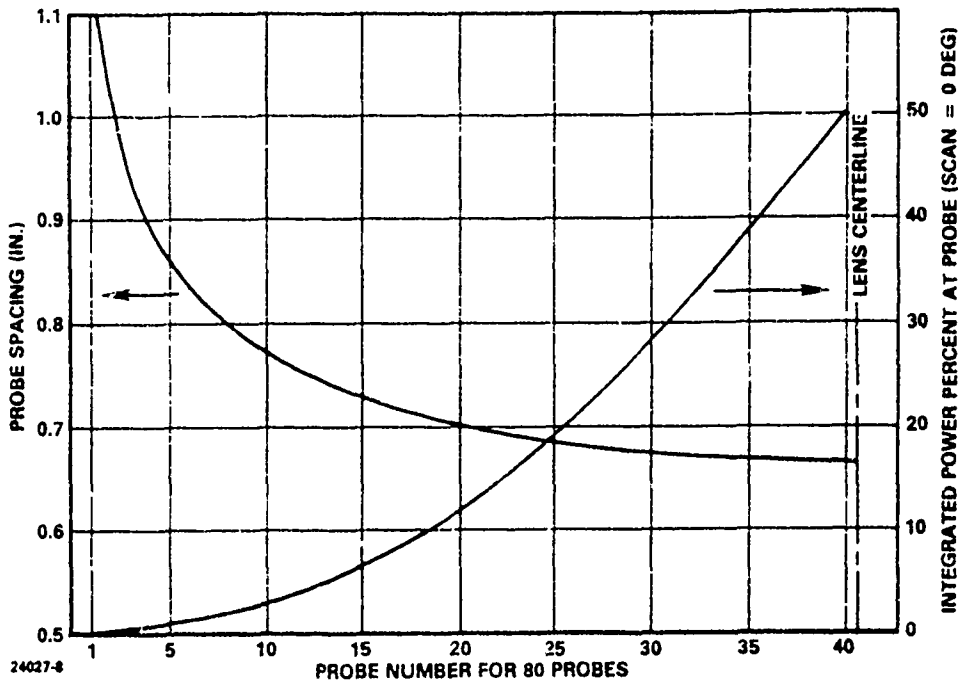


Figure 7 - Probe Spacings

probes at 40 deg could establish a grating lobe and that only 1 to 2 percent of the total energy would be incident on those probes. Moreover, Figure 8 shows that the spacing of the edge probes is rapidly varying, and the periodicity of the spacing is nonexistent. This led to the conclusion that any grating lobe effects would be negligible.

A waveguide simulator was used to match the probes in an array environment. Inspection of Figure 3 will show that a probe matched over a range of incidence angles of 0 to 35 deg would cover virtually all probes of a ± 30 -deg scan region. The waveguide simulator in Gustincic³ simulates the operation of a probe in an infinite array by consideration of the TE₁₀ mode in waveguide as composed of two plane waves with incidence angle θ given by

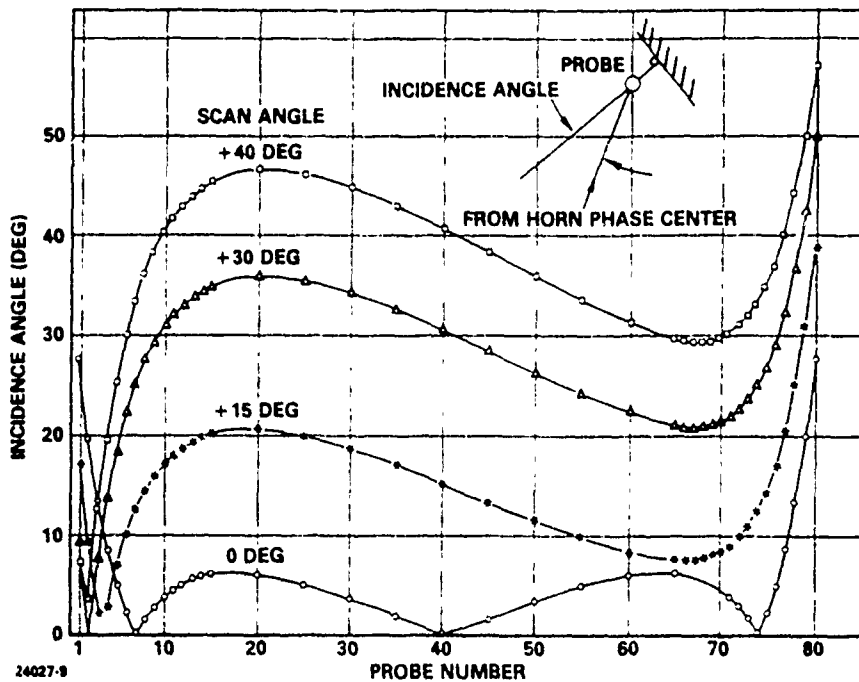


Figure 8 - Probe Incidence Angle from Horn

$$\sin \theta = \frac{\lambda}{2a} \quad (2)$$

where a is the guide width. In theory any angle of incidence can be simulated, provided higher order modes are suppressed and the probe spacing being simulated is maintained by use of multiple probes when required.

The probe was matched to a VSWR of under 1.10 at an incidence angle of 31 deg by adjustment of the distance between the probe and the end short plate, and by addition of a capacitive button to the probe tip. Incidence angles less than 31 deg were expected to also have an acceptable VSWR.

The bootlace cables are standard UT-141 semirigid with solid dielectric. A number of alternates were considered, but all were either too expensive to offset any performance improvements, were supplied only in

precut lengths with connectors attached, or did not exhibit good phase stability during environmental testing.

Good phase stability in the selected cable was achieved by an initial heating of the cables to an elevated temperature, trimming off the extruded teflon, and attachment of the SMA connectors. Additional tests over a wide range of temperatures demonstrated that the cable phase could be controlled to better than 3 deg using this technique.

4.2.3 Lens Folding - A major obstacle to be overcome in the implementation of the lens fed array was accommodation of the parallel plate propagation region within the antenna envelope. For acceptable phase deviation and scan angle results, a lens $F/D \cong 0.7$ was required, which posed a space factor problem. The most acceptable solution to this problem was to fold the parallel plates. However, the bend introduced by folding creates a phase shift which will be dependent on the angle of incidence, θ_i , at the bend. Because θ_i will be both probe number and scan angle dependent, compensation will be difficult. Calculations showed that, for a ± 30 -deg scan, θ_i will vary from 0 to 30 deg for probes near the lens center, and from 30 to 70 deg for edge probes. The largest differential change is on the order of 40 deg.

Computation of the phase shift was made by two methods. The first used equations in Marcuvitz⁴ for an E-plane waveguide bend, with changes in θ_i made by adjustment of the waveguide width. The second method (Bahar⁵) required solving the wave equation in cylindrical coordinates.

Because the bend angle can assume any angle, the solution requires Hankel functions of real, non-integer order.

The two solutions are compared in Figure 9 for a 180-deg E-bend with a 1-in. centerline bend radius and 0.5-in. plate separation. The agreement is well within acceptable tolerances, and Marcuvitz⁴ equations were subsequently incorporated into the lens design computer program.

Several approaches to fabricating the folded parallel plates were investigated. The approach which best met the requirements of low weight, low propagation loss, structural integrity and intraplate alignment without intraplate support, was a precision assembly of 10 aluminum numerically-controlled machinings. Alignment is controlled through the inner

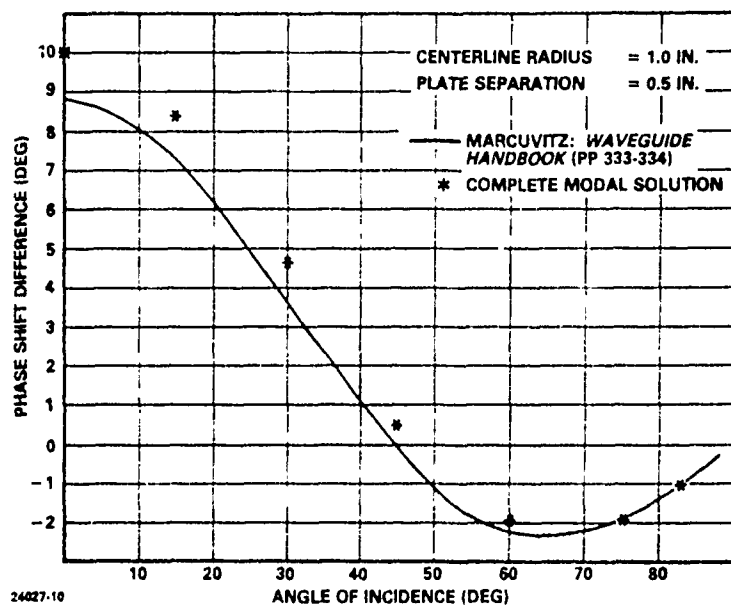


Figure 9 - Phase Shift Difference Between Unfolded and Folded Parallel Plate at 180-Deg E-Plane Bend

and outer bend sections and the end caps which tie them together. The flat plate sections bolt to the bends with close tolerance tongue and groove joints ensuring alignment. An optimum balance between weight and structural integrity was achieved by machining a quilted pattern on the outer surfaces, thereby incorporating integral structural stiffeners. Plate thickness between the structural stiffeners was reduced to 0.020 to 0.030 in.

4.2.4 Feed Horn - A conventional H-plane flared horn with a 2- by 0.4-in. aperture was used as the lens feed. Quarter-wave chokes were used to reduce radio frequency (RF) breakdown potential between the horn and the parallel plates. Teflon buttons on both top and bottom of the horn worked as a low-friction contact and centering mechanism between the plates.

Initial lens calculations used a theoretical H-plane horn pattern. After selection of the 2-in. aperture was made, a number of horn patterns were measured in a parallel plate and used to further refine the calculated performance.

Feed horn positioning required special attention. A search for a suitable means of position sensing led to a device known as the Inductosyn, manufactured by Farrand Controls. The Inductosyn provides highly precise linear position sensing and permits the position sensing to be accomplished directly at the feed horn. The Inductosyn consists of a stationary printed circuit approximately 0.5-in. wide extending the length of the feed horn track, a sensing element which mounts to the feed horn, and remote electronics. The overall closed loop horn positioning accuracy is on the order of ± 0.004 in., which is equivalent to a worst-case angular uncertainty

of ± 1 arc minute (0.017 deg). The Inductosyn was chosen over comparable optical sensors because of its tolerance to accumulated surface contaminants as well as its tolerance to wide temperature excursions.

Another aspect of the feed horn positioning problem is the design of a transmission line connection between the roll axis rotary joint (the antenna system input) and the feed horn which is capable of accommodating the wide range of feed horn motion. High power handling capability, low loss, and reliability were the governing design considerations. The approach followed which produced excellent results was an articulating waveguide assembly made up of two movable waveguide sections connected to each other and to the horn and stationary input waveguide by three rotary joints.

The feed horn mounts to a hardened V-groove track via rollers. The feed horn track is concentric with the focal arc and is positioned so that the feed horn phase center falls on the focal arc. The feed horn is positioned by a servoloop consisting of a steel tape drive band connected to a DC torque motor with the Inductosyn providing the loop error signal. The loop electronics are contained in a separate antenna control unit located remote from the antenna.

4.3 Array Design -

4.3.1 Waveguide Radiator - The radiator is an open-ended waveguide. The dimensions are shown in Figure 10 and were analyzed using Diamond's⁶ infinite array analysis. The computed E-plane scan admittance normalized to the waveguide is also shown in Figure 10.

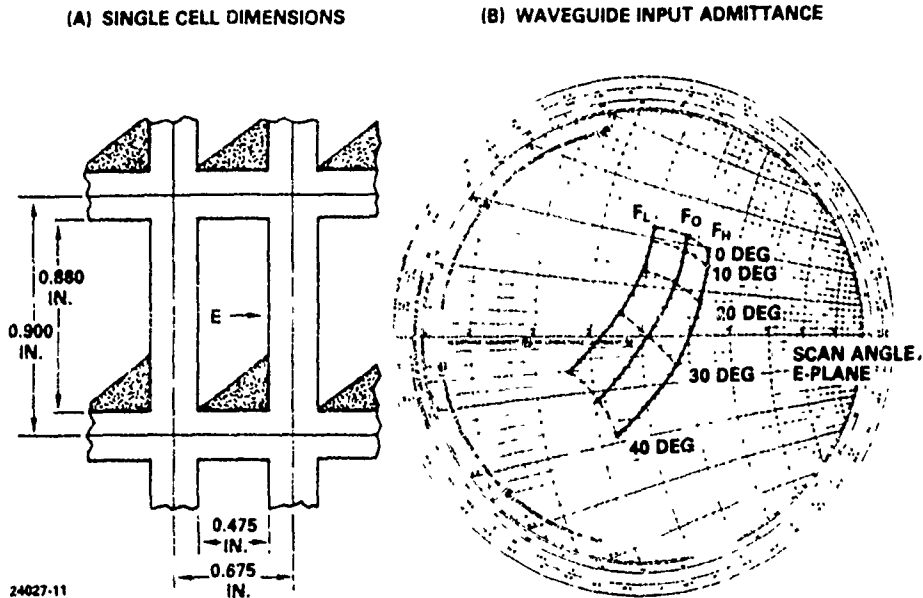
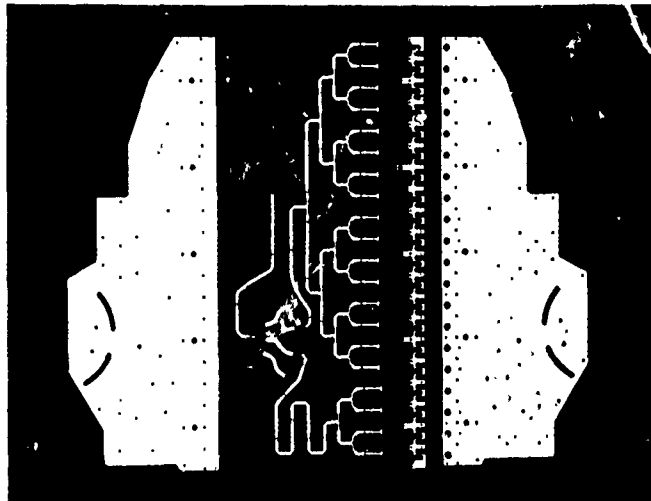


Figure 10 -- Waveguide Infinite Array Admittance

4.3.2 Vertical Radiating Assembly - Selection and design of the vertical radiating assembly involved a significant part of the total antenna design effort. Because the antenna contained 80 of the assemblies, weight and total cost of the design would be critical to overall antenna success. In addition, total insertion loss must also be minimized.

Each vertical assembly contained 20 open-ended waveguide radiators, an airstrip power divider with an integral stripline to waveguide transition, a three-way stripline mechanical switch, and the coax to stripline input connector. The assembly is shown in exploded form, minus the airstrip-to-switch card finger contacts, in Figure 11.

Mechanical design of the array addressed several objectives. It was desired that the array have inherent structural integrity and that it contribute to the basic structural stiffness of the entire antenna assembly with



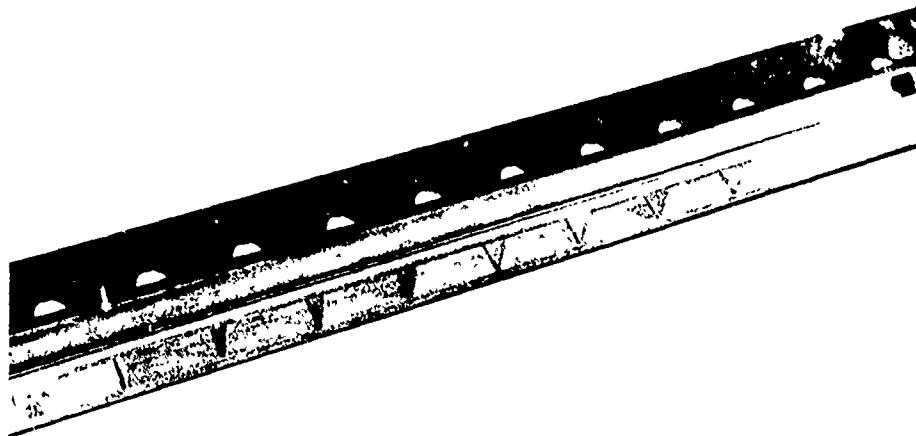
24027-12

Figure 11 – Vertical Power Divider Assembly

a minimum of additional structure. Assembly of the array should be straightforward with a minimum of fixturing or specialized alignment and fitting techniques. Weight and cost were to be minimized.

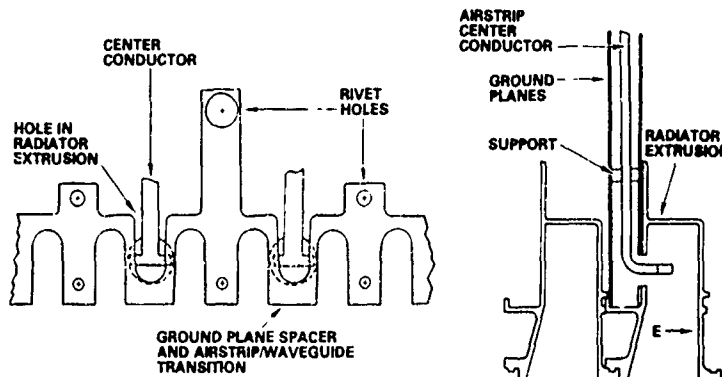
The answer to these objectives was found to lie in the design of a three-sided, thin-walled aluminum extrusion with an interlocking edge design. The open-ended waveguide elements are formed by dip brazing aluminum partitions into the extrusion at appropriate intervals to provide a single vertical element of the array. The interlocking edge feature satisfies the ease of assembly criterion and contributes to the goal of inherent structural integrity. Low cost and weight are inherent in the use of an extrusion.

A waveguide assembly, including partitions and holes drilled for alignment, assembly, and the waveguide-to-stripline transition is shown in Figure 12. Mechanical relationship of adjoining extrusions, waveguide-to-stripline transition, and spacer is shown in Figure 13.



24027-13

Figure 12 - Radiator Assembly



24027 14

Figure 13 - Waveguide to Power Divider Assembly

4.3.3 Elevation Power Divider - The elevation power divider is balanced stripline with air dielectric. Ground plane spacing is 0.200 in. and the rectangular center conductor is 0.050-in. thick.

Design of the T-junctions was largely empirical, as published data is not accurate for cases where the center conductor width and thickness becomes an appreciable fraction of a wavelength. The use of high quality test fixtures and an automated network analyzer for removal of test set

errors was found to be essential. In addition, all dimensions established in the laboratory had to be checked using end mills and cutters representative of those to be used in production, to optimize performance on a unit-to-unit basis.

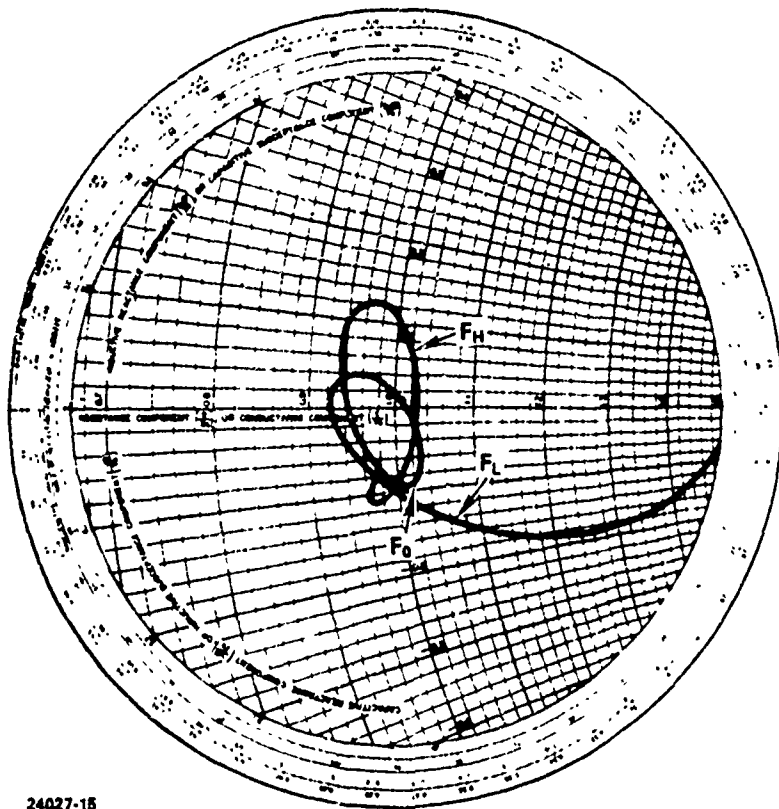
The center conductor is supported by nylon spacers with a small pin through the center conductor. The capacitive effect of the pin was compensated for by a reduction in the conductor width over a total length of approximately $\lambda/4$. The number and location of the standoffs was based upon a vibration analysis and an allowable deviation of the center conductor from a centered location between the ground planes.

The stripline to waveguide transition is an integral part of the stripline. After machining, the T-shaped adapter is bent at a right angle and inserted through a hole in the waveguide wall. A spacer bar both spaces the ground planes and provides a square coax section in the vicinity of the transition to suppress higher order modes.

Measured VSWR of a 16-port power divider, including the stripline to waveguide transition, is shown in Figure 14. Similar data was obtained on the four-port divider.

4.3.4 Elevation Beam Switch - A mechanically movable stripline card is used to select one of three elevation beams. Contact between the card and the power divider center conductor is through beryllium copper fingers.

A torque motor and shaft is used to actuate the switches. A lever arm connects each card to the shaft, and the card is constrained in lateral movement by nylon rollers located between the ground planes.



24027-15

Figure 14 - Sixteen-Port Power Divider Admittance

The beryllium copper fingers represented a significant experimental design effort to realize a design capable of maintaining contact over board variations in thickness, warpage, and deflections, while at the same time providing acceptable VSWR and insertion loss at an acceptable manufacturing price.

Measured VSWR of the switch card, including fingers and airstrip support posts located next to the card, was under 1.15 in all positions.

An additional factor was the angular positional accuracy of the card relative to the fingers. Tests showed that misalignment of ± 0.020 in. was acceptable.

To date the switches have been actuated several hundred times with no evidence of degradation. This has included operation during an environmental test simulating a typical aircraft pod.

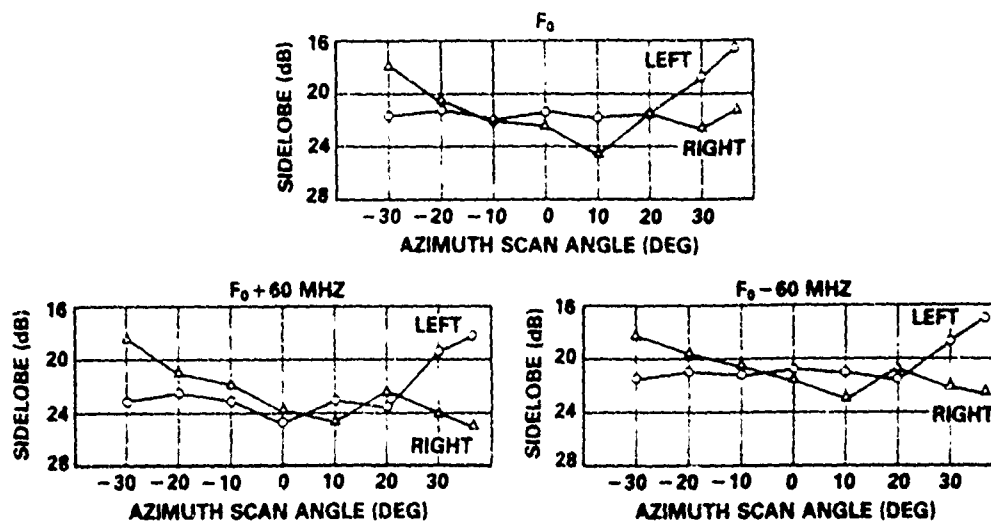
4.3.5 Pressure Cylinder - A requirement for pressurization is imposed by transmitter peak power levels and operation in an unpressurized pod at high altitudes. The impracticality of pressurizing the basic antenna is evident when the problem of sealing the feed horn access to the parallel plate region is addressed. Pressure containment was achieved by enclosing the antenna in a thin-wall composite cylinder having good microwave transmission as well as excellent structural and temperature properties.

5. ANTENNA PERFORMANCE

This antenna was tested on a 2250-ft range. Both transmit and test antennas are about 35 ft above flat terrain. The range has been used for production X-band antenna testing for about eight years, and has measured amplitude ripples over a 4-ft-high by 8-ft-wide aperture of 0.5 dB maximum.

Peak azimuth sidelobes for three frequencies and a scan angle of +38 to -30 deg are shown in Figure 15 for the 20-port switch position. Very similar data was measured for the 16-port and four-port positions.

Antenna gain loss, measured at the feed horn for zero-deg scan, ranged from -2.4 to -3.0 dB, relative to the theoretical aperture gain. An additional 0.9 dB of loss occurred in three azimuth and one roll axis rotary joints, and over 5 ft of connecting waveguide. Typically, scanning to 30 deg introduced an additional 0.5 dB of loss, with 0.7 dB at 38 deg.



24027-16

Figure 15 - Peak Azimuth Sidelobes

Typical azimuth and elevation patterns are shown in Figures 16 through 22. A full ± 90 -deg azimuth cut is shown in Figure 22. Overall falloff of the lobes is excellent out to about 45 deg, but relatively high lobes are present in the 45- to 70-deg region. These lobes vary in amplitude, but in general are present for all scan angles measured. Their cause was not established, but could be due to an illumination error over the lens probes or to reflections caused by extraneous structure around the antenna mount.

Because a Rotman lens is a wideband device, data was measured at a frequency 10 percent above the center design frequency. Despite known mismatches in the elevation power divider, the beam switch, and the lens, no azimuth or elevation pattern degradations were measured. More importantly, little or no change in beam position was measured, further confirming the suitability of a lens as a wideband, widescan antenna.

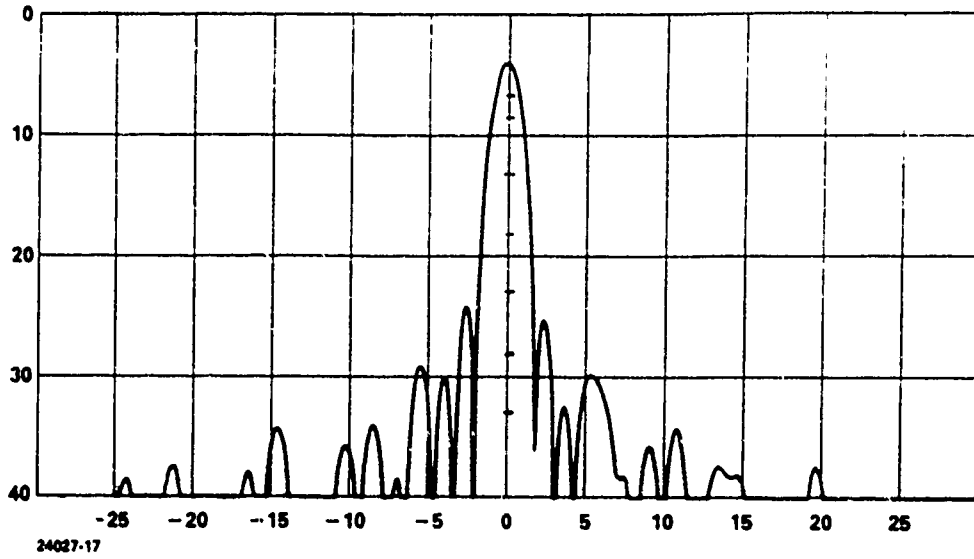


Figure 16 - Zero-Deg Scan, Frequency = F_0 , Azimuth Cut

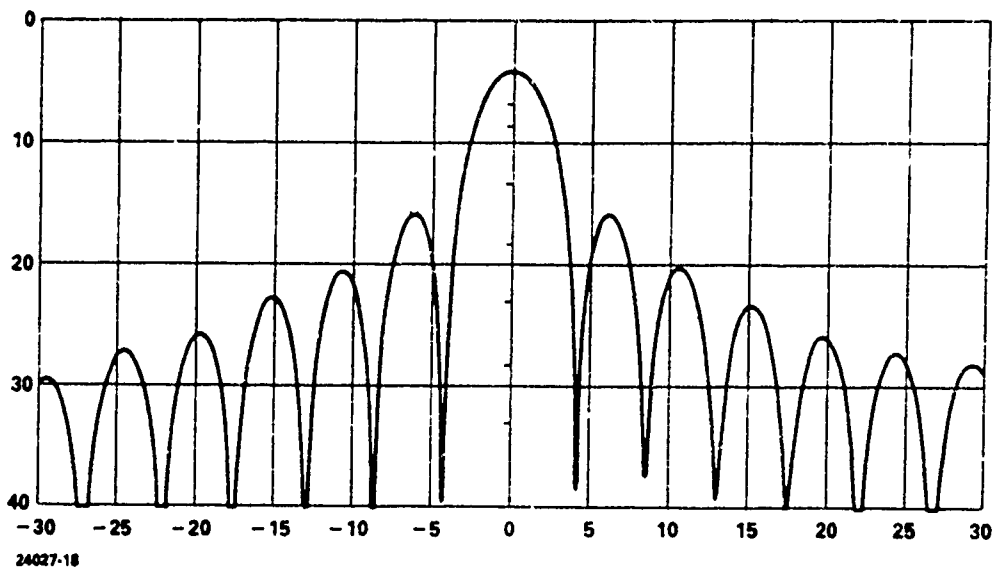


Figure 17 - Zero-Deg Scan, Frequency = F_0 , Elevation Cut

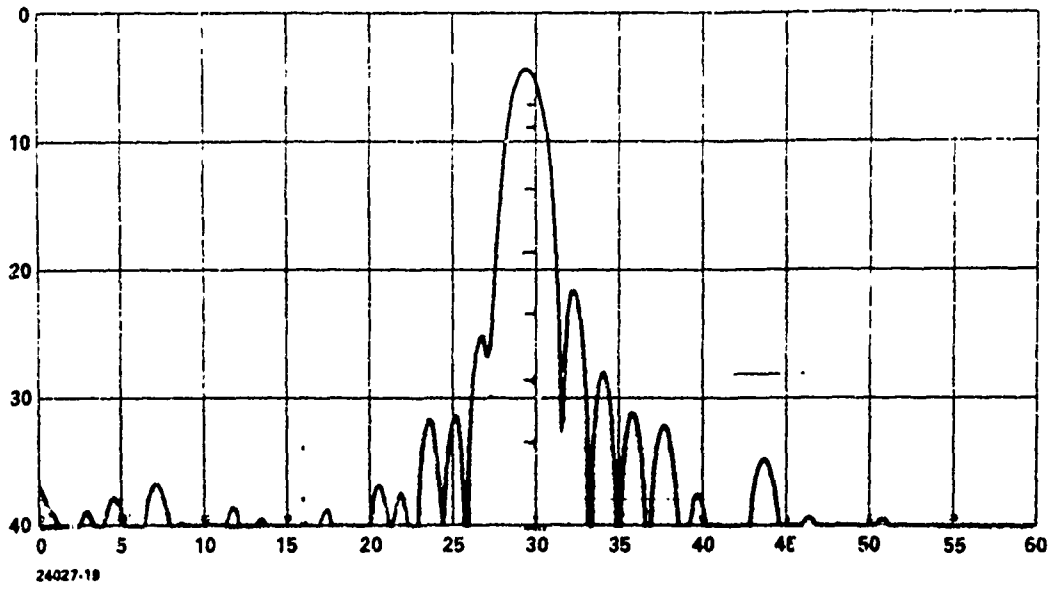


Figure 18 - Thirty-Deg Scan, Frequency = F_0 , Azimuth Cut

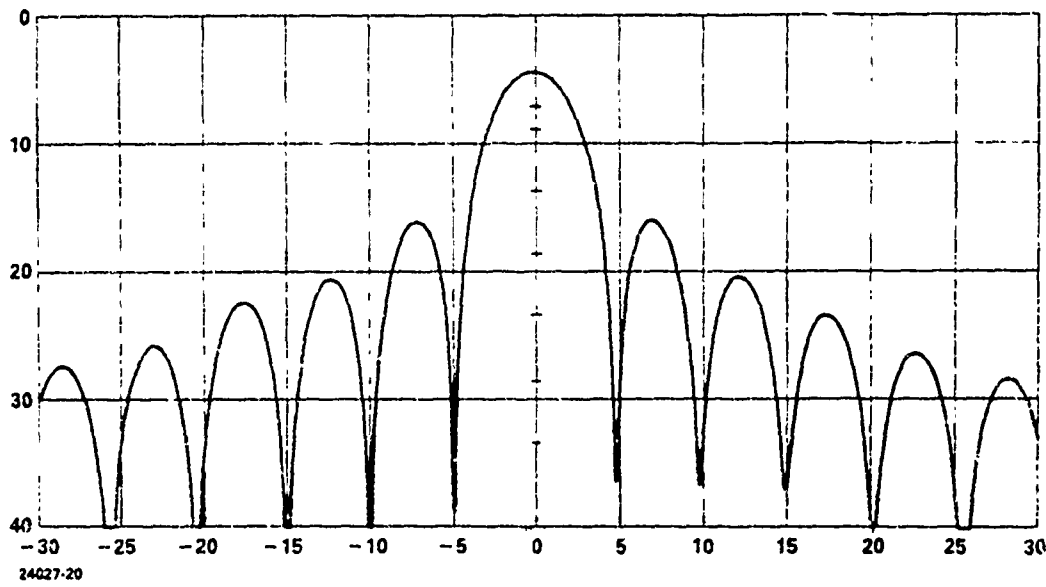


Figure 19 - Thirty-Deg Scan, Frequency = F_0 , Elevation Cut

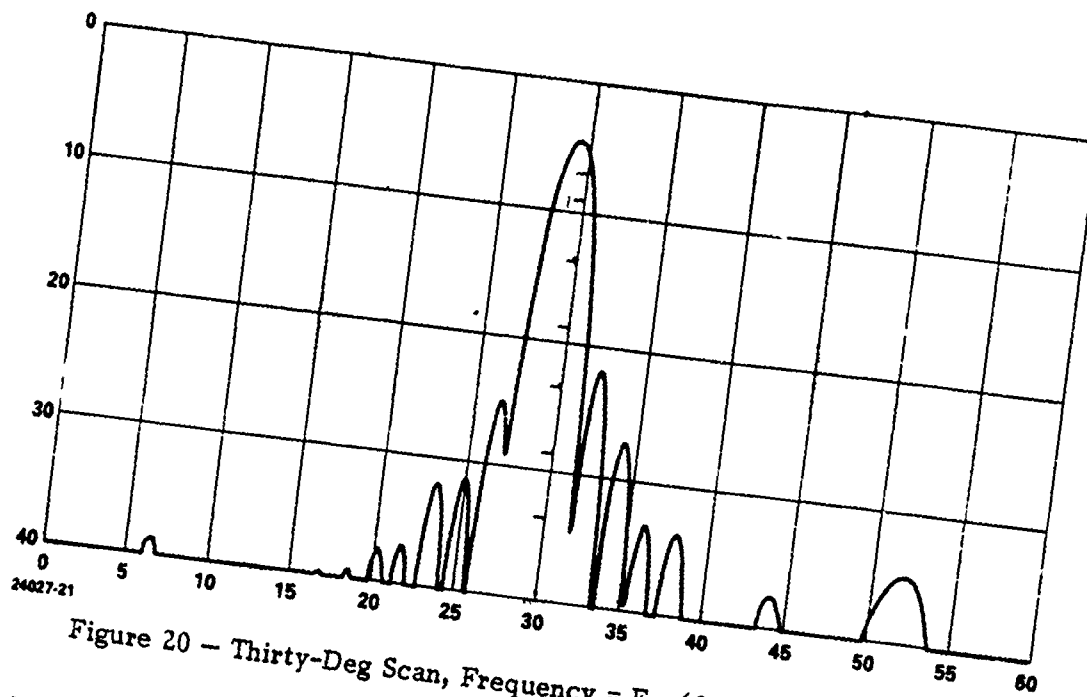


Figure 20 - Thirty-Deg Scan, Frequency = $F_0 - 60$ MHz, Azimuth Cut

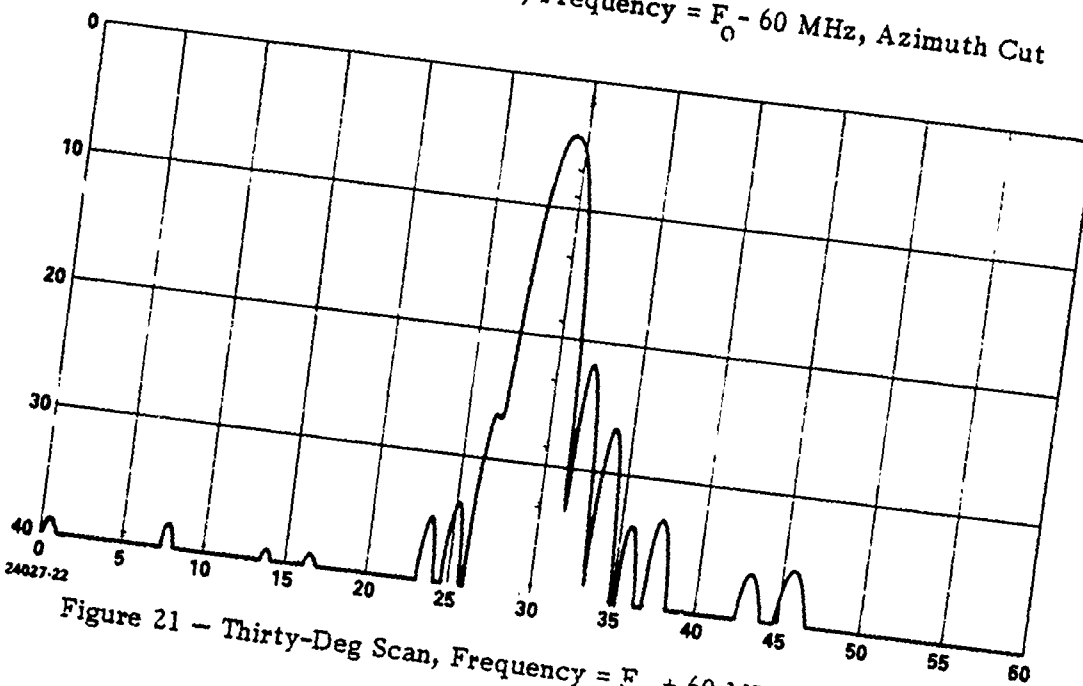


Figure 21 - Thirty-Deg Scan, Frequency = $F_0 + 60$ MHz, Azimuth Cut

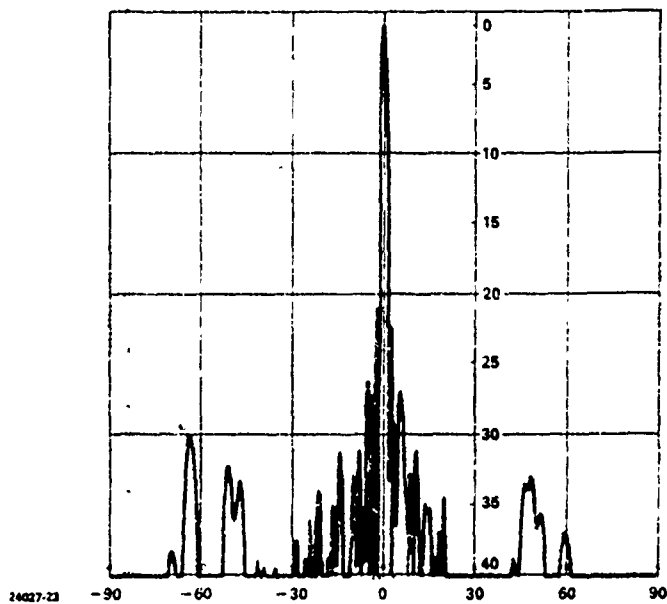


Figure 22 - Zero-Deg Scan, Frequency = F_0 , Full ± 90 -Deg Azimuth Cut

6. PRODUCIBILITY

A major concern throughout the development effort was producibility of the antenna on a moderate to large scale as well as the immediate single unit fabrication. This concern is reflected in several aspects of the mechanical design. In particular, components of the vertical radiators and power dividers were designed with production quantities in mind. Both the ground planes and the circuits of the power divider networks are capable of being fabricated by precision stamping although quantities involved in the prototype did not warrant the expenditure for tooling. The extrusion approach to the vertical radiators is another example of a manufacturing technique suitable for volume production.

Assembly was addressed again in the area of the multi-element array. The interlocking edge feature of the vertical radiators and the repeating

planar nature of the power dividers both contributed to a simple stacking assembly procedure which did not rely on complex fixturing or highly skilled personnel.

7. SUMMARY

This paper has described a wideband, wide scan antenna with application to pod-mounted reconnaissance radars. A folded lens as a performance effective alternate to a phase shifter scanned array has been demonstrated. A key to the overall success of the antenna was a philosophy which emphasized minimal weight, producibility, and suitability for production during all stages of development. The design is expected to be readily adaptable to specific program requirements.

8. ACKNOWLEDGEMENTS

A number of people contributed to the success of this antenna by contributing ideas, moral support, and hard work. In particular, W.C. Woody provided invaluable ideas and concepts for the overall antenna design; W.O. Klever served as project lead engineer; H.A. Burger developed the vertical power divider and switch; A.C. Brown, Jr. provided the parallel plate bend and probe analysis; B.W. McIntyre provided a consistently high level of laboratory data; and R.E. Meyer led the mechanical design team and shepherded the antenna through the fabrication, assembly, and test phases. Their contributions are gratefully acknowledged.

REFERENCES

1. Ruze, J. (1950) Wide-angle metal-plate optics, Proc. IRE Vol 38:53.
2. Rotman, W. and Turner, R.F. (1963) Wide-angle microwave lens for line source applications, IEEE Trans. Vol AP-11:623.
3. Gustincic, J.J. (1972) The determination of active array impedance with multielement waveguide simulators, IEEE Trans. Vol AP-20:589.
4. Marcuvitz, N. (1950) Waveguide Handbook, McGraw-Hill, New York, p. 333.
5. Bahar, E. (1969) Fields in waveguide bands expressed in terms of coupled local annular waveguide modes, IEEE Trans.-MTT, Vol 17:210.
6. Diamond, B.L. (1968) A generalized approach to the analysis of infinite planar array antennas, Proc. IEEE Vol 56:1837.

